Marine Pollution Bulletin 167 (2021) 112284

Contents lists available at ScienceDirect

Marine Pollution Bulletin

journal homepage: www.elsevier.com/locate/marpolbul

Spatiotemporal variation, speciation, and transport flux of TDP in Leizhou Peninsula coastal waters, South China Sea

Peng Zhang [a], Peidong Dai [a,b], Jibiao Zhang [a,*], Jianxu Li [a], Hui Zhao [a], Zhiguang Song [a]

[a] College of Chemistry and Environmental Science, Guangdong Ocean University, Guangdong, Zhanjiang 524088, China
[b] Guangzhou Chinese Academy of Sciences Test Technical Services, Co., Ltd., Guangdong, Guangzhou 510000, China

ARTICLE INFO

Keywords:
TDP
Spatiotemporal variation
Speciation
Transport flux
Leizhou Peninsula coastal waters

ABSTRACT

Phosphorus (P) plays key role in phytoplankton primary production in coastal water. In this study, seawater samples collected within China's Leizhou Peninsula coastal waters from October 2017 to July 2018 were examined to determine the seasonal variation, speciation, and transport flux of total dissolved phosphorus (TDP) linked to hydrographic features. TDP concentration and speciation had significant seasonal variations ($P < 0.01$), and the annual mean TDP concentration was 0.42 ± 0.25 μmol·L^{-1}. High concentrations of TDP occurred in coastal waters adjacent to Zhanjiang Bay and Jianjiang River estuary, whereas low TDP concentrations were found across large offshore areas. Dissolved inorganic and organic P were the main TDP bulk species in different seasons, comprising up to 55.5 ± 7.9% and 46.5 ± 22.6%, respectively. The Beibu Gulf was annually subjected to 3.5 × 10^9 mol flux of TDP through the Qiongzhou Strait. Coastal currents, river plumes, and human activities were responsible for the dynamic variations in P species.

1. Introduction

Phosphorus (P), one of the most important nutrients needed by all living organisms, can control primary productivity in estuarine and marine environments (Anderson et al., 2002; Benitez-Nelson, 2000; Karl and Björkman, 2001; Lin et al., 2013). Total dissolved phosphorus (TDP) is an essential nutrient for the growth of marine primary and secondary producers (Conley et al., 2009; Duan et al., 2016; Glibert, 2017; Hansell and Carlson, 2014). TDP occurs in both dissolved inorganic phosphorus (DIP) and dissolved organic phosphorus (DOP) (Lin et al., 2012; Loh and Bauer, 2000; Shi et al., 2015). The DIP pool consists of orthophosphate (PO_4^{3-}), pyrophosphate (pyroP), and polyphosphate (polyP). PO_4^{3-}, the dominant form, has high reactivity and can be utilised easily by phytoplankton, whereas pyroP and polyP cannot be absorbed easily by some phytoplankton species (Bjorkman and Karl, 1994; Diaz et al., 2016; Lin et al., 2013; Xu et al., 2008). Algae and bacteria can utilise DOP compounds as a source of P nutrition in marine environments (Bjorkman and Karl, 1994; Fang, 2004; Fang and Wang, 2020; Kolowith et al., 2001). Biogeochemical processes such as uptake, remineralisation, and physical and biological exchanges among these various pools are the essential components of the marine P cycle (Duan et al., 2016; Fox et al., 1986; Hansell and Carlson, 2014; Li et al., 2017). In coastal waters, investigations of carbon (C) and nitrogen (N) have been much more comprehensive than those of TDP speciation and fluxes, which are less well-documented (Hansell and Carlson, 2014).

The continental shelf is well-known for its high biological productivity, due to abundant nutrients derived from land via river discharge and/or supplied through coastal upwelling and shoreward cross-shelf transport (Boynton et al., 1995; Conley et al., 1995; Fang, 2004; Howarth et al., 1995; Yang et al., 2018). In addition, coastal waters are active interfaces between terrestrial and oceanic environments with large discharges of fluvial materials, complex biogeochemical processes, and anthropogenic inputs (Cai et al., 2012; Canton et al., 2012; Fang and Wang, 2020; Faul et al., 2005; Meng et al., 2015). Anthropogenic influences on coastal water, such as increased land reclamation, agricultural fertilisation, livestock, and urban/industrial wastewater inputs, have significantly changed TDP concentrations in coastal waters over the last three decades (Fang, 2000; Hansell and Carlson, 2014; Lin et al., 2013; Yang et al., 2018). Improved knowledge of P species dynamics in coastal water systems is needed to better understand the biogeochemical

Abbreviations: P, phosphorus; TDP, total dissolved phosphorus; DIP, dissolved inorganic phosphorus; DOP, dissolved organic phosphorus; LZP, Leizhou Peninsula; SCS, South China Sea; LZQNYH, Leizhouqingnianyunhe; LZPCW, Leizhou Peninsula Coastal Water; GDWCW, Guangdong Western Coastal Water; GDWCC, Guangdong Western Coastal Current; QZSCW, Qiongzhou Strait Coastal Water; BBGCW, Beibu Gulf Coastal Water.

* Corresponding author.
E-mail address: zhangjb@gdou.edu.cn (J. Zhang).

https://doi.org/10.1016/j.marpolbul.2021.112284
Received 17 June 2020; Received in revised form 12 March 2021; Accepted 14 March 2021
Available online 23 March 2021

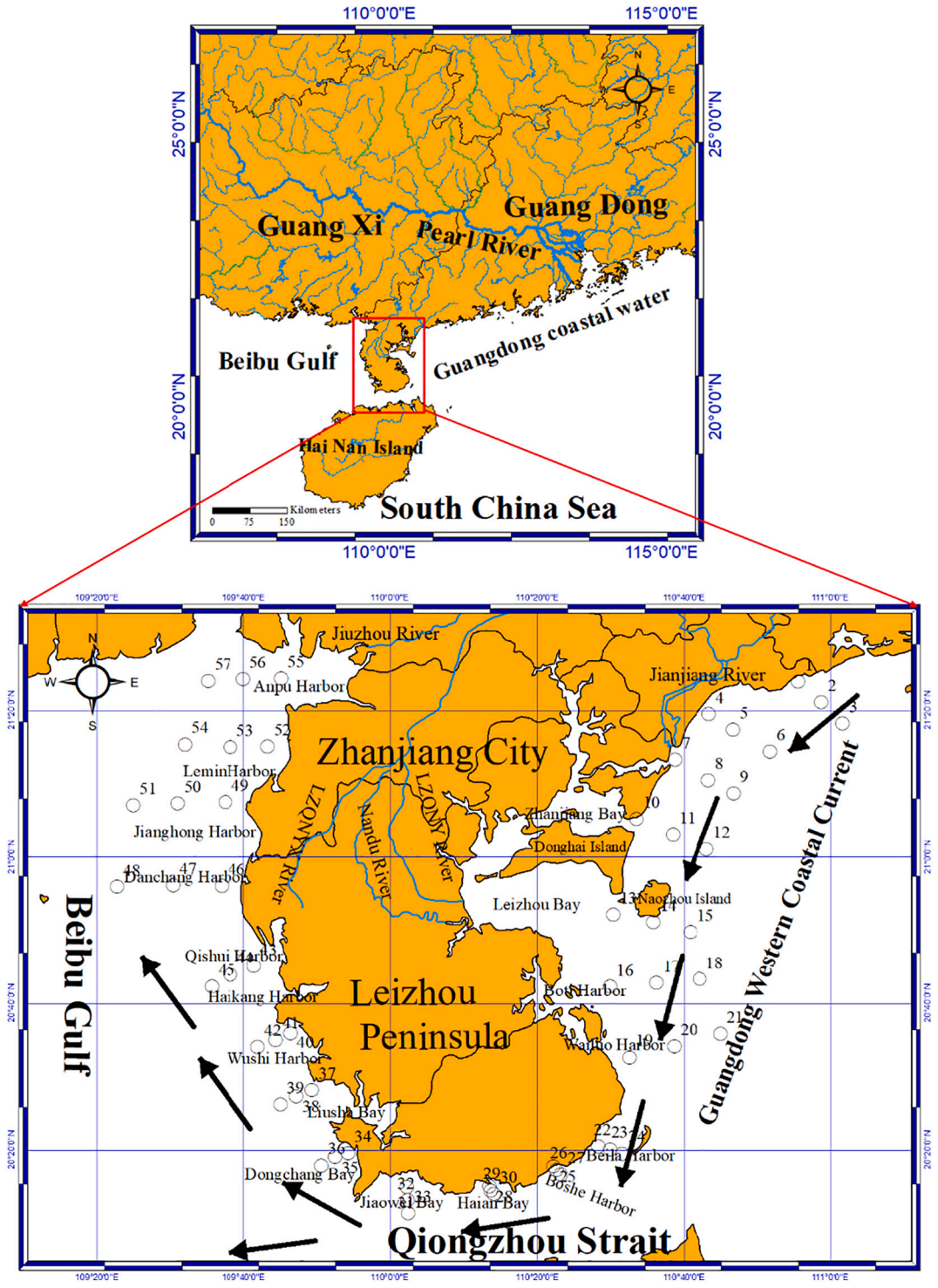

Fig. 1. Study area, monitoring station locations, and water currents in the Leizhou Peninsula coastal water (LZPCW).

cycling of P and its role in regulating water and environmental quality in these environments (Boesch et al., 2009; Dagg et al., 2007; Meng et al., 2015).

The Leizhou Peninsula (LZP), located in Guangdong Province (Fig. 1) between Hainan Island and the northern Beibu Gulf (BBG), is the biggest peninsula in South China, covering an area of 8888 km^2 with a coastline 1450 km long (Li et al., 2014). The Leizhou Peninsula Coastal Water (LZPCW) can be divided into three water bodies based on geographic features: the Guangdong Western Coastal Water (GDWCW), the Qiongzhou Strait Coastal Water (QZSCW), and the Beibu Gulf Coastal Water (BBGCW) (Fig. 1). The LZPCW, a semi-closed marginal sea and one of the world's most representative shallow continental shelf oceans, is rich in natural resources and plays an important role in human life and economic exploitation within the South China Sea.

In terms of coastal water hydrodynamics, the QZSCW also forms a link for water, material, and energy exchange between the BBGCW and GDWCW. Coastal currents carry mass westward most of the time, but change to eastward movement during monsoon season (Bao et al., 2005; Gao et al., 2017; Shi et al., 2002; Yang et al., 2014). The Guangdong Western Coastal Current (GDWCC) plays an important role in mass

transport, water quality maintenance, and aquaculture in the waters near western Guangdong and the BBG (Bao et al., 2005; Xie et al., 2012; Yang et al., 2015). In addition, seasonal variations in Pearl River estuarine coastal plumes can impact nutrient dynamics in the GDWCW (Fu et al., 2020; Pang, 2006; Xu et al., 2008; Yang et al., 2014). Such river plumes are loaded with carbon, nutrients, and sediments, meaning that their interactions with coastal circulations significantly affect the shelf's hydrographical features and biogeochemistry (Cai et al., 2004; Dai et al., 2014; Xu et al., 2008). Thus, the LZPCW is a dynamic system governed by riverine inputs, coastal currents, and anthropogenic activities. Though regarded as one of China's less-developed coastal areas, environmental contamination and degradation in this area are evident. At present, relatively few studies have assessed P speciation and exchange through the QZSCW, while studies examining the seasonal variation, distribution, and speciation of both DIP and DOP and their links to hydrographical features in the LZPCW are even scarcer.

Therefore, this paper investigated inorganic and organic P variation, speciation, and transport flux in the LZPCW from 2017 to 2018 based on four field observations in order to (1) explore spatiotemporal distribution patterns of TDP; (2) identify spatiotemporal speciation patterns of TDP; and (3) estimate the seasonal TDP transport flux between the west and east coasts of the LZPCW. The results provide baseline data for future research on P biogeochemical processes and coastal environmental management in the LZPCW.

2. Materials and methods

2.1. Study area

The LZPCW is a dynamic coastal region characterised by complex physical processes (Fig. 1). Tidal waves, which are dominated by diurnal constituents on the western side and by semidiurnal constituents on the eastern side, propagate toward the QZS from the BBG and decrease significantly in amplitude within the strait (Shi et al., 2002). The QZS is a remarkable example of a long, narrow, shallow, and strongly stratified strait with bidirectional water mass exchanges (Gao et al., 2017; Shi et al., 2002). There are many estuaries, bays, and ports along the LZPCW (Fig. 1), which have played a key role in the development of Zhanjiang's marine economy. Zhanjiang city has the largest marine aquaculture area in Guangdong coastal water, with the area 6.5×10^4 ha in 2016 (Zhang et al., 2020a). The QZS influences the hydrography and biogeochemistry of the BBGCW, Hainan offshore coastal waters, and the GDWCW. The exchange flow rates of the GDWCW and BBGCW toward the BBG during most of the year are significant factors affecting circulation in the South China Sea.

2.2. Monitoring stations and sampling

Seawater samples were collected from 57 sampling sites in the LZPCW in October 2017 (autumn), January 2018 (winter), May 2018 (spring), and July 2018 (summer) using the research vessel *Tianlong* (Fig. 1). During sampling, seawater was collected from the surface, middle, and bottom (0.5 m above sediment) layers. Monitoring stations 1–21 were located in the GDWCW, stations 22–33 were located in the QZS (between the GDWCW and BBGCW) to characterise the QZSCW, and stations 34–57 were located in the BBGCW to characterise seawater in the BBG.

Seawater samples were collected by a CTD-Rosette system using Teflon-coated bottles (10 L, Sea Bird Inc., USA). Data for temperature (T) and salinity (S), were continuously determined by temperature- salinity probes during the field investigation (China National Standardization Management Committee, 2007). Immediately after collection, for P (TDP) determination, ~1 L seawater was filtered through pre-acid-cleaned and pre-combusted (450 °C for 4 h) 47 mm diameter glass fibre filters (GF/F). In this study, the dissolved and particulate forms of P in coastal water were determined by the 0.45 μm Nuclepore filter (Lin et al., 2013). The filtrate samples for TDP and DIP were collected in acid-cleaned HDPE bottles and stored at −20 °C until laboratory analysis, respectively.

2.3. Measurements TDP species

Measured P species included DIP, DOP. Concentrations of TDP (DIP + DOP) were measured using an oven-assisted acid persulfate method (Grasshoff et al., 1999) with some modifications (Lin et al., 2012). In short, 10 mL of the water sample was first mixed well with 1 mL of acidified $K_2S_2O_8$ solution (50 g/L, pH = 1) in a Teflon vial, then digested in an oven at 120 °C for 4 h. After digestion, the TDP concentration was measured by the standard phosphomolybdenum blue method using a visible spectrophotometer (Koroleff, 1983; Grasshoff et al., 1999). DIP concentrations were directly measured without digestion. DOP concentrations were calculated from the difference between TDP and DIP. Standard solutions were treated as samples during sample processing and analysis to ensure data quality. The detection limit was 8–10 nM based on replicate blank sample measurements, with a precision better than 2% for both DIP and TDP. Accuracy of TDP was assured using the standard addition method of calibration with recoveries of 94–101%, and RSD of both repeatability and reproducibility of <5% (Grasshoff et al., 1999; Zhang et al., 2021).

2.4. Spatiotemporal TDP species transport flux calculation

The spatiotemporal TDP species transport fluxes were calculated using the following procedures. TDP species export was estimated from the GDWCW, representing the P fluxes from the GDWCW to the BBGCW with water discharge data. The seasonal TDP species exchange between the GDWCW and the BBGCW was estimated by multiplying the water flux by the TDP species concentration in the net inflow seawater. In previous study, the mean water flow is determined by the seasonal average of residual currents at each monitoring stations (Shi et al., 2002). The synthetic analysis of all current data available over the last 37 years shows that there is a year-round westward mean flow in QZS (Shi et al., 2002). Thus, the seasonal mean water discharge data was estimated based on the on a cross-strait transect with an average width of 29.5 km and an average depth of 46 m. In addition, the seasonal mean TDP species (stations 22–33 in the Fig. 1) was used to estimate the P transport flux in QZSCW. Therefore, seasonal TDP fluxes transported were used to quantify from the GDWCW to the BBGCW. The seasonal and annual fluxes of TDP species used here were estimated as:

$$F_{TDP} = C_{TDP} \times Q_{TDP} \quad (1)$$

where F_{TDP} is the seasonal flux of TDP speciation in QZSCW, C_{TDP} is the average concentration of TDP species in coastal water during that each season ($\mu mol \cdot L^{-1}$), and Q_{TDP} is the cumulative discharge of coastal water ($m^3 \cdot d^{-1}$).

2.5. Statistical analysis

Pearson correlation analysis with a two-tailed test of significance was performed using the IBM SPSS Statistics 20 programme to study the relationship between the measured parameters. SPSS was also used to run one-way analysis of variance (ANOVA) to examine the statistical differences in data between two or more groups. Correlation between variables was determined by Pearson correlation between the environmental factors and coastal water quality using SPSS 22.0. A probability level of 0.05 was used to determine significance.

Table 1
Seasonal temperature and salinity data from the LZPCW.

Location	Parameters	Parameters	Annual	Spring	Summer	Autumn	Winter
LZPCW	T (°C)	Mean	26.3 ± 5.2	27.3 ± 0.9	29.0 ± 0.5	30.1 ± 0.6	18.7 ± 0.7
		Range	17.5–31.5	26.1–28.8	28.1–30.5	25.0–31.5	17.5–20.6
	S (‰)	Mean	31.2 ± 1.2	31.3 ± 0.9	32.3 ± 0.7	29.5 ± 2.5	31.8 ± 1.2
		Range	24.7–33.5	29.6–31.8	27.7–33.1	24.7–32.9	28.4–33.5

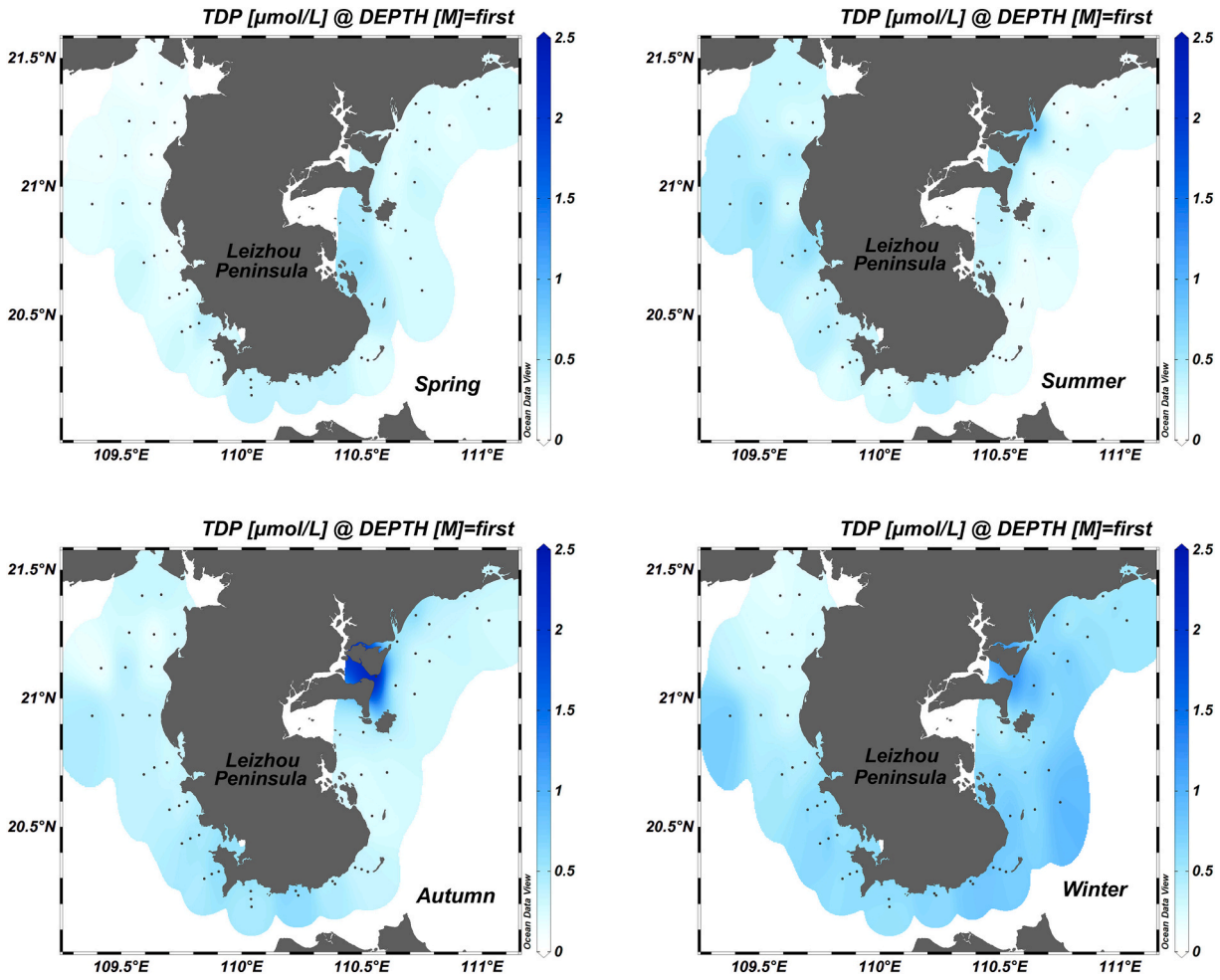

Fig. 2. Spatiotemporal variations in TDP concentrations.

3. Results

3.1. Hydrographic features

The seasonal mean T (water temperature) and S (salinity) varied significantly in the LZPCW ($P < 0.01$). T ranged from 17.5–31.5 °C (average 26.3 ± 5.2 °C) while S ranged from 24.7–33.5‰ (average 31.2 ± 1.2‰) (Table 1). Autumn had the highest T values (30.1 ± 0.6 °C), while average summer and spring T values were slightly lower (29.0 ± 0.5 °C and 26.3 ± 5.2 °C, respectively) and average winter T values were the lowest (18.7 ± 0.7 °C). S values were highest in summer (32.3‰), while average winter and spring S values were slightly lower (31.8‰ and 31.3‰, respectively) and average autumn S values were lowest (29.5‰).

3.2. Spatiotemporal variations in TDP

The mean TDP concentrations showed significant differences in seasons ($P < 0.01$) (Fig. 2). TDP concentrations in the LZPCW ranged from 0.05–3.21 μmol·L^{-1} (average 0.42 ± 0.25 μmol·L^{-1}), increasing from autumn to winter, decreasing in spring, and slightly increasing in summer; the maximum and minimum values occurred in autumn and summer, respectively (Table 2). The spatial distribution of TDP concentrations in the LZPCW also varied significantly (Fig. 2). In all seasons, high concentrations of TDP in the LZPCW occurred in coastal waters adjacent to Zhanjiang Bay and the mouth of the Jianjiang River in the GDWCW, whereas low TDP concentrations were found across large offshore areas. In autumn, TDP concentrations ranked from GDWCW > QZSCW > BBGCW, while in winter and spring these ranked from QZSCW > GDWCW > BBGCW in winter and spring (Table 2). In comparison, these values increased from GDWCW < QZSCW < BBGCW in summer.

3.3. Spatiotemporal patterns of TDP species

3.3.1. DIP

DIP concentrations in LZPCW surface seawater revealed seasonal and spatial differences ($P < 0.01$) (Fig. 3). The DIP concentration ranged

Table 2
Seasonal mean and range of DIP, DOP, and TDP concentrations in the LZPCW (μmol·L^{-1}).

Stations	Speciation	Parameters	Spring	Summer	Autumn	Winter
All Coastal waters	TDP	Mean	0.28 ± 0.09	0.33 ± 0.14	0.44 ± 0.36	0.60 ± 0.19
		Range	0.10–0.57	0.05–0.85	0.15–3.21	0.19–1.23
	DIP	Mean	0.14 ± 0.06	0.17 ± 0.10	0.19 ± 0.18	0.40 ± 0.18
		Range	0.04–0.34	0.00–0.55	0.00–1.62	0.00–0.90
	DOP	Mean	0.13 ± 0.07	0.15 ± 0.08	0.25 ± 0.21	0.20 ± 0.12
		Range	0.01–0.36	0.02–0.36	0.03–1.59	0.00–0.68
	DOP/TDP	Mean	46.5 ± 19.5	48.6 ± 19.9	56.8 ± 20.9	35.2 ± 24.6
		Range	11.4–82.3	10.8–100.0	10.8–100.0	0.7–100.0
GDWCW	TDP	Mean	0.28 ± 0.08	0.23 ± 0.14	0.51 ± 0.62	0.64 ± 0.19
		Range	0.19–0.57	0.05–0.85	0.19–3.21	0.19–1.23
	DIP	Mean	0.12 ± 0.05	0.11 ± 0.10	0.17 ± 0.30	0.44 ± 0.16
		Range	0.04–0.30	0.00–0.55	0.04–1.62	0.00–0.90
	DOP	Mean	0.17 ± 0.07	0.13 ± 0.07	0.34 ± 0.33	0.20 ± 0.15
		Range	0.02–0.34	0.02–0.30	0.11–1.59	0.01–0.68
	DOP/TDP	Mean	58.5 ± 16.5	55.4 ± 20.5	70.5 ± 7.9	31.8 ± 21.3
		Range	11.8–82.3	11.8–100.0	49.6–85.2	1.6–100.0
QZSCW	TDP	Mean	0.34 ± 0.06	0.30 ± 0.09	0.45 ± 0.12	0.71 ± 0.11
		Range	0.19–0.43	0.15–0.48	0.24–0.71	0.52–0.85
	DIP	Mean	0.17 ± 0.07	0.18 ± 0.07	0.25 ± 0.08	0.51 ± 0.09
		Range	0.09–0.34	0.04–0.30	0.13–0.34	0.30–0.68
	DOP	Mean	0.16 ± 0.04	0.12 ± 0.06	0.21 ± 0.10	0.20 ± 0.11
		Range	0.09–0.25	0.03–0.26	0.04–0.37	0.05–0.38
	DOP/TDP	Mean	49.2 ± 12.8	40.7 ± 17.2	44.4 ± 15.8	27.2 ± 13.2
		Range	20.6–70.4	10.9–78.0	10.8–66.5	10.2–47.7
BBGCW	TDP	Mean	0.24 ± 0.10	0.41 ± 0.10	0.39 ± 0.12	0.51 ± 0.18
		Range	0.10–0.57	0.15–0.62	0.15–0.62	0.24–0.90
	DIP	Mean	0.15 ± 0.05	0.22 ± 0.10	0.18 ± 0.10	0.32 ± 0.19
		Range	0.04–0.26	0.04–0.38	0.00–0.34	0.00–0.64
	DOP	Mean	0.09 ± 0.07	0.19 ± 0.08	0.20 ± 0.10	0.19 ± 0.11
		Range	0.01–0.36	0.02–0.36	0.03–0.39	0.00–0.55
	DOP/TDP	Mean	35.2 ± 18.2	46.8 ± 19.3	54.0 ± 24.2	42.0 ± 28.5
		Range	11.4–70.9	10.8–87.3	10.9–100.0	0.0–100.0

from 0.00–1.62 μmol·L^{-1} (average 0.23 ± 0.18 μmol·L^{-1}), increasing from autumn to winter, decreasing in spring, and slightly increasing in summer (Table 2). The spatial distribution of DIP concentrations in the LZPCW showed significant variations and had a similar trend to TDP, decreasing in an offshore direction (Fig. 3). In all seasons, high DIP concentrations occurred in coastal waters adjacent to Zhanjiang Bay and the mouth of the Jianjiang River in the GDWCW, whereas low DIP concentrations were found across large offshore areas. In autumn, DIP concentrations ranked from QZSCW > BBGCW > GDWCW (Table 2), while in winter and spring these ranked from QZSCW > GDWCW > BBGCW. In comparison, these values increased from GDWCW < QZSCW < BBGCW in summer.

3.3.2. DOP

DOP concentrations in LZPCW surface seawater revealed seasonal and spatial differences ($P < 0.01$). The DOP concentration ranged from 0.00–1.59 μmol·L^{-1} (average 0.18 ± 0.14 μmol·L^{-1}), decreasing from autumn to winter, decreasing further in spring, then slightly increasing in summer (Table 2). The spatial distribution of DOP concentrations in the LZPCW showed significant variations (Fig. 4) and had a similar trend to TDP, decreasing in an offshore direction. In all seasons, high DOP concentrations occurred in coastal waters adjacent to Zhanjiang Bay and the mouth of the Jianjiang River in the GDWCW, whereas low DOP concentrations were found across large offshore areas (Fig. 4). In autumn, DOP concentrations ranked from GDWCW > QZSCW > BBGCW (Table 2), while in winter and spring these ranked from QZSCW > GDWCW > BBGCW. In comparison, these values increased from GDWCW < QZSCW < BBGCW in summer.

3.3.3. Spatiotemporal variation of TDP speciation

TDP speciation in LZPCW seawater revealed seasonal and spatial differences ($P < 0.01$) (Fig. 5). The DOP/TDP ranged from 0.7–100.0% (average 46.5 ± 22.6%) (Fig. 5), significantly decreasing from autumn to winter, increasing in spring, then slightly increasing in summer (Table 2). The spatial distribution of DOP/TDP in the LZPCW showed significant variations (Fig. 5). In autumn and summer, DOP/TDP ranked from GDWCW > BBGCW > QZSCW (Table 2) while in winter this ranked from BBGCW > GDWCW > QZSCW. In comparison, this increased from BBGCW < QZSCW < GDWCW in spring.

3.4. Seasonal TDP transport flux between west and east coast of LZPCW

The calculated TDP fluxes in the QZSCW showed that fluxes of TDP species entering the BBGCW varied significantly by season ($P < 0.01$). The annual flux of TDP discharged into the BBG was 3.5 × 10^9 mol, while the total fluxes of TDP in spring, summer, autumn, and winter were 7.7 × 10^8 mol, 4.3 × 10^8 mol, 7.0 × 10^8 mol, and 1.6 × 10^9 mol, respectively (Fig. 6). The seasonal transport fluxes of TDP, DIP, and DOP had similar trends. TDP speciation fluxes were highest in winter, lower in spring and autumn, and lowest in summer. The transport flux of DIP was greater than DOP, and DIP was the predominant form of the transport TDP pool in the water column. The annual transport fluxes of DIP and DOP accounted for 62% and 38%, respectively.

4. Discussion

4.1. Comparison with global TDP concentration and speciation data

Owing to the gradient of chemical properties of coastal water, such as pH, S, dissolved oxygen, suspended particulate matter and hydrodynamic conditions, the biogeochemical process of P is rather complex under various anthropogenic impacts in coastal water ecosystem (Fang and Wang, 2020; Zhang et al., 2021). The TDP speciation concentrations in the LZPCW were comparable to values reported elsewhere for coastal waters around the world. The average LZPSCW TDP concentration (0.41 ± 0.14 μmol·L^{-1}) was lower than that of the Yellow Sea (Duan et al., 2016), East China Sea (Fang, 2004), and Pearl River Estuaries in China (Li et al., 2017), but higher than that of the eastern North Pacific

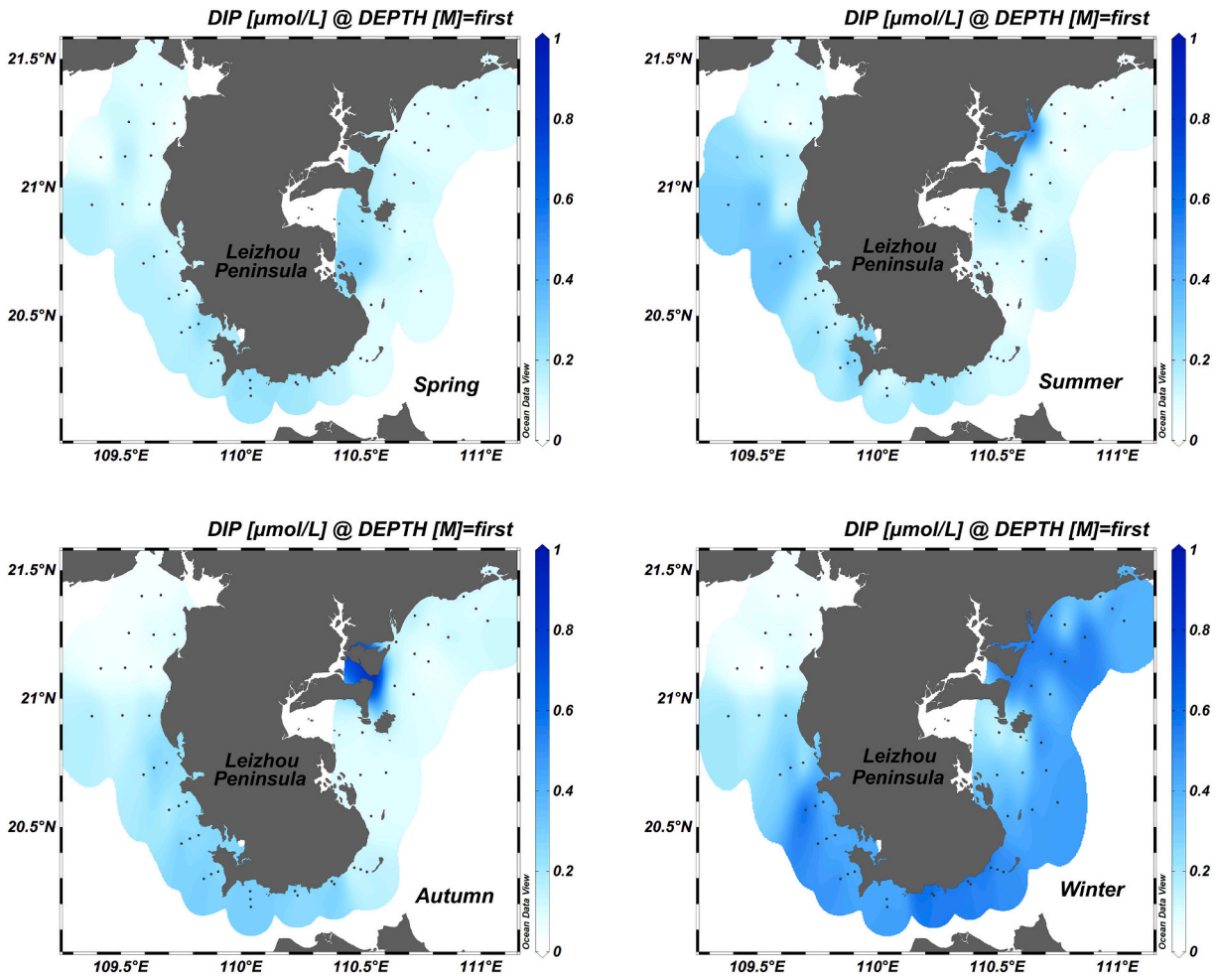

Fig. 3. Spatiotemporal variations in DIP concentrations.

Ocean (Loh and Bauer, 2000), the subtropical Atlantic Ocean (Mather et al., 2008), the north-western Mediterranean Sea (Raimbault et al., 1999), and the north-eastern Pacific Ocean off Mexico (Orrett and Karl, 1987), where were not greatly affected by human activities, reflecting human disturbance in the LZPCW (Yang et al., 2018; Zhang et al., 2021). Within the LZPCW TDP pool, the DOP abundance was slightly lower than that for DIP, consistent with previous observations in the southern subtropical Atlantic Ocean and eastern North Pacific Ocean, where DIP was the predominant P species (Mather et al., 2008). However, this was significantly distinct from the Bohai Sea (Liu et al., 2011), Yellow Sea (Duan et al., 2016), northern subtropical Atlantic Ocean (Mather et al., 2008), north-western Mediterranean Sea (Raimbault et al., 1999), and north-eastern Pacific Ocean off Mexico (Orrett and Karl, 1987) (Table 3). Due to the strong fixation of P in the natural soils, the higher DIP abundance may be attributed to the enriched P land-based runoff from the over agricultural P fertilizer application in LZP (Du et al., 2004). Compared with the BBGCW in the summer of 2006, DOP/TDP (46.8 ± 8.9%)was significantly lower than those coastal waters in BBG (73%), which could be attributed to differences in seawater monitoring stations offshore of the BBGCW (Jiang et al., 2008). Similar results were found between the inner shelf and open shelf of the East China Sea (Fang, 2004) and in the Danshui and Scheldt estuaries (Fang and Wang, 2020; van der Zee et al., 2007). The DOP concentration exceeded that of DIP and became the dominant fraction in TDP at S values >25‰ (Fang and Wang, 2020). It may be attributed to phytoplankton production because the higher DOP concentration was generally accompanied with a higher Chl-a concentration (Fang and Wang, 2020).

4.2. *Hydrographic factors affecting spatiotemporal TDP variations*

Seasonal hydrographic factors (T and S) in the LZPCW affected spatiotemporal variations in TDP (Fig. 7), significantly influencing its concentration and speciation (Table 4). In the GDWCW, there was a significant positive correlation between TDP and temperature in spring, summer, and winter ($P < 0.01$) and a negative correlation in autumn ($P < 0.01$) that may have been caused by higher T restricting phytoplankton growth and primary production (Eppley, 1972). In addition, there was a distinct negative correlation between TDP species and S in summer ($P < 0.01$), indicating that TDP species in coastal waters were mainly derived from the transport of terrigenous nutrients (Zhang et al., 2019b). In summer, the freshwater discharge was highest, although the Pearl River estuarine coastal plume turned eastward upon exiting the Pearl River estuary due to the south-westerly monsoon (Dai et al., 2014; Xu et al., 2008). The mean annual freshwater input from the Pearl River was ~3260 × 10^8 m^3 with >70% of freshwater discharged in flood season (Pang, 2006). In addition, many other rivers along the LZP's and Hainan island coast influenced TDP's spatiotemporal distribution (Zhang et al., 2019a; Zhang et al., 2020b). Because there are some small riverine nutrients input along LZP's and Hainan Island coastline (Zhang et al., 2020a, 2020b; Zhang et al., 2021).

In the QZSCW, there was a positive correlation between TDP and S during spring and autumn ($P < 0.01$), possibly induced by coastal water incursions from the BBG, as the BBGCW contained a northward current off the western coast of Hainan Island during these seasons (Gao et al., 2017). In addition, as the QZS forms an active channel between Guangdong and Hainan Island, human activities, such as aquaculture

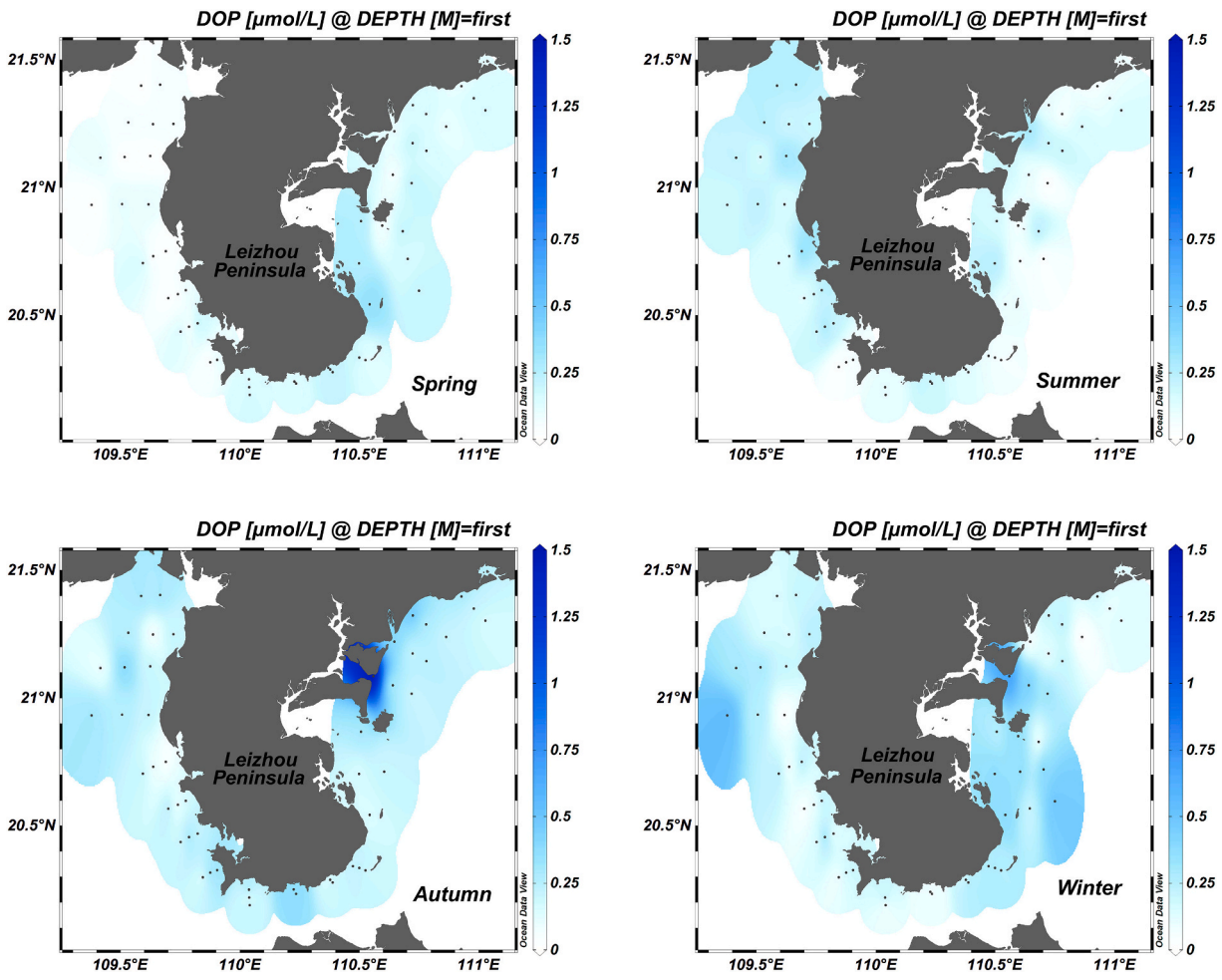

Fig. 4. Spatiotemporal variations in DOP concentrations.

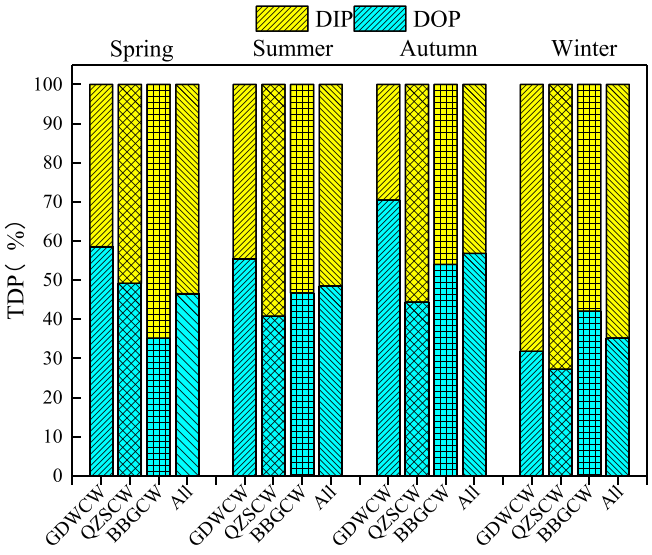

Fig. 5. Spatiotemporal composition of TDP.

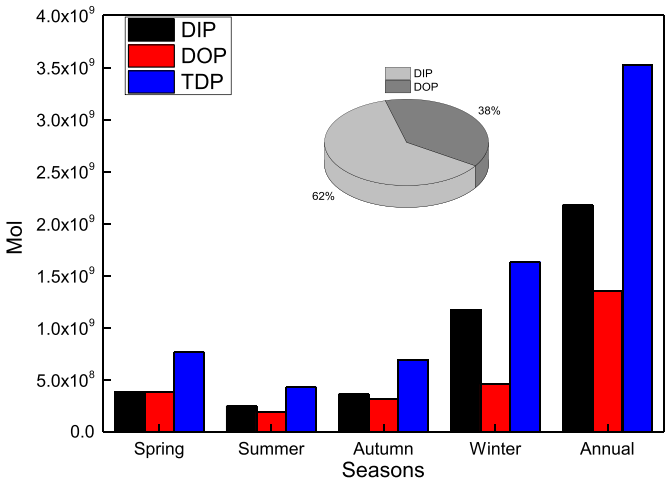

Fig. 6. Seasonal fluxes of TDP speciation discharge from the QZS into the BBG.

and waste water discharge have a certain influence on the nutrient distribution in adjacent coastal water (Zhang et al., 2019a). Furthermore, some high P concentration diffusion in coastal waters adjacent to Hainan Island also impacted TDP species, such as Haikou city adjacent coastal water with high DIP concentration (Zhang et al., 2019a; Zhang et al., 2020b).

In the BBGCW, there was a significant negative correlation between TDP, DIP, and T in spring ($P < 0.01$), but no significant correlation between DOP and T ($P > 0.05$), because DIP was the major fraction of TDP (64.8%). Most coastal waters were affected by land-based sources, such agricultural fertilizer utilization and livestock culture in LZP.

Table 3
DIP, DOP, and TDP concentrations and their partitioning in TDP pools around the world.

Study area	DIP μmol·L^{-1}	DOP μmol·L^{-1}	TDP μmol·L^{-1}	DOP/TDP %	Reference
Eastern North Pacific Ocean	0.26	0.229	0.489	47	Loh and Bauer, 2000
Bering Sea	0.9 ± 0.47	0.0 ± 0.11	0.99	11 ± 15	Lin et al., 2012
Northern subtropical Atlantic Ocean	0.009	0.08	0.089	90	Mather et al., 2008
Southern subtropical Atlantic Ocean	0.21	58	0.15	42	Mather et al., 2008
Bohai Sea 2008 (08–09)	0.07–0.22	0.19–0.27	0.26–0.50	60–70	Liu et al., 2011
Yellow Sea 2012 (09)	0.19	1.03	1.22	83	Duan et al., 2016
East China Sea, inner shelf 2001 (03)	0.56 ± 0.11	0.13 ± 0.04	0.69	19%	Fang, 2004
North Atlantic Scotian Shelf	0.34	0.14	0.48	29	Ridal and Moore, 1990
Southern California Bight	0.20	0.21	0.41	51	Ammerman and Azam, 1985
North-western Mediterranean Sea	0.007	0.13	0.137	95	Raimbault et al., 1999
North-eastern Pacific Ocean off Mexico	0.124	0.126	0.191	66	Orrett and Karl, 1987
Pearl River Estuary	1.44 ± 0.57	0.58 ± 0.42	2.02	29%	Li et al., 2017
BBGCW 2006 (07–08)	0.32	0.86	1.18	73%	Jiang, 2008
LZPCW 2017–2018	0.23 ± 0.12	0.18 ± 0.05	0.41 ± 0.14	46.5 ± 22.6	This study

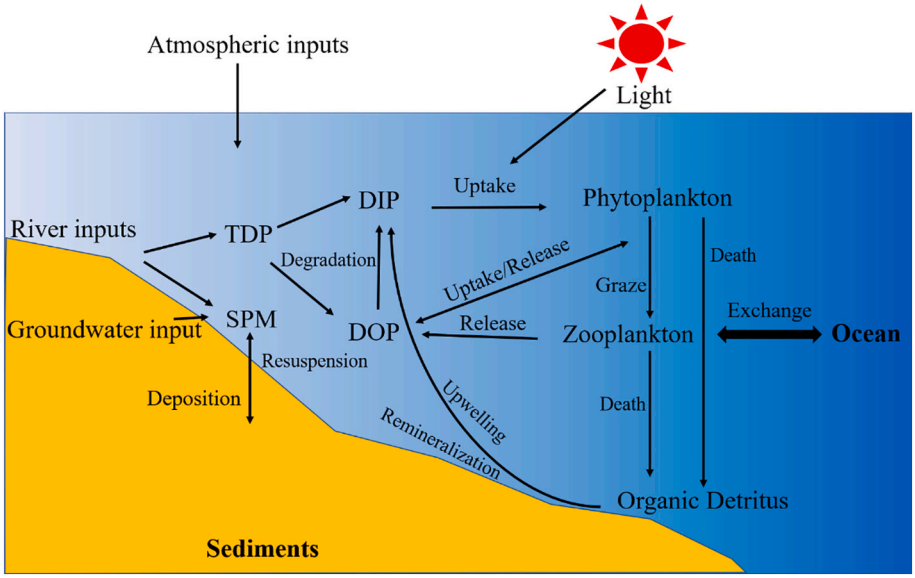

Fig. 7. Schematic representation of TDP biogeochemical processes in the coastal zone.

Table 4
Pearson coefficients between TDP speciation concentration and T and S in the LZPCW.

Area	Season	TDP		DIP		DOP	
		T	S	T	S	T	S
GDWCW	Spring	0.469**	0.053	0.224	0.041	0.414**	0.035
	Summer	0.475**	−0.729**	0.424**	−0.722**	0.345*	−0.432**
	Autumn	−0.649**	0.212	−0.761**	0.187	−0.526**	0.228
	Winter	0.388**	0.158	0.281	0.045	0.197	0.154
QZSCW	Spring	−0.388	0.494*	−0.585**	0.611**	0.322	−0.210
	Summer	0.203	−0.055	0.023	−0.064	0.262	−0.005
	Autumn	−0.276	0.564**	−0.092	0.794**	−0.277.	0.069
	Winter	−0.015	0.209	0.141	0.216	−0.126	0.038
BBGCW	Spring	−0.519**	0.368*	−0.586**	0.381**	−0.273	0.220
	Summer	−0.102	0.065	0.328*	0.122	−0.525**	−0.064
	Autumn	0.059	0.383**	0.125	0.669**	−0.058	−0.236
	Winter	0.015	0.575**	−0.002	0.628**	0.028	−0.173

* Correlation is significant at $P < 0.05$ (two-tailed).
** Correlation is significant at $P < 0.01$.

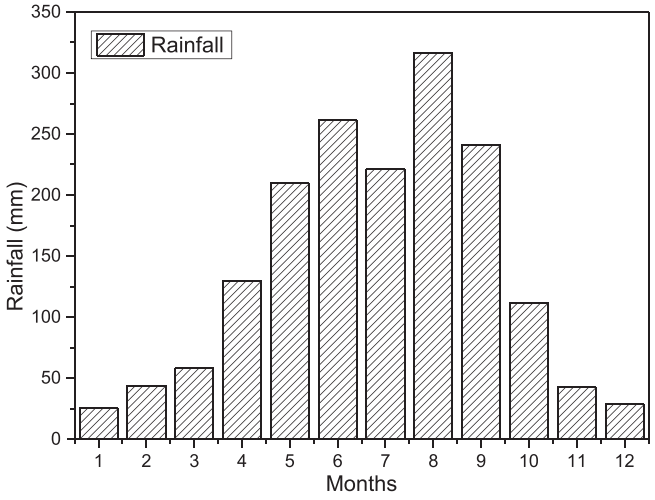

Fig. 8. Monthly mean rainfall in Zhanjiang from 1981 to 2010 (China Meteorological Data Service Centre, 2020).

Increased T in coastal waters means that DIP can be better absorbed by phytoplankton and bacteria. Moreover, in summer, T had a significant positive and negative correlation between DIP and DOP, respectively, but there was no significant correlation between TDP and T, indicating that the transformation process between DIP and DOP was controlled by T in summer. Because the assimilation rate of DIP by phytoplankton and the remineralisation rate of DOP by bacteria was equivalent (Duan et al., 2016; Karl and Björkman, 2001). Thus, the T may indirectly regulate interactions between DIP by phytoplankton and bacteria activities. Additionally, S had positive correlations between TDP and DIP in all seasons except for summer ($P < 0.01$). This may have been caused by P sources from marine aquaculture emissions via the few river influences in the western LZP (Guo et al., 2019; Xu et al., 2021), but BBGCW self-circulation could also lead to the release of DIP/DOP from sediment into coastal waters (Dagg et al., 2004; Froelich, 1988; Huang and Zhang, 2010).

4.3. Input sources affecting spatiotemporal TDP variations

Riverine nutrients entering the LZPSCW had a significant influence on spatiotemporal TDP variations (Fig. 7). There was a distinct negative correlation between TDP and salinity in western Guangdong in summer ($P < 0.01$), indicating that TDP in coastal waters mainly originated from the transport of terrestrial nutrients in summer (Table 4). This likely relates to the fact that monthly rainfall was highest in summer (Fig. 8). In summer, the TDP flux was the largest in high water flow which induced by rainfall (Zhang et al., 2021). Rivers along the LZP's coast include the LZQNY River, Jiuzhou River, Jianjiang River, and other small rivers, with large freshwater and suspended sediment fluxes. The Jianjiang River produces a freshwater flux of 76.82×10^8 $m^3 \cdot year^{-1}$ and 1.80×10^6 $t \cdot year^{-1}$ of suspended sediment (Zhanjiang City Government, 2013). After entering the LZPCW, TDP form in this freshwater would be carried westward by currents in the GDWCW, resulting in the higher DIP, DOP, and TDP found at adjacent coastal waters.

In addition, some eutrophic bays and estuaries affected spatiotemporal TDP variations, such as Zhanjiang Bay, Liusha Bay, and Anpu Harbour. Hot-spots of TDP distribution were identified in all seasons in coastal waters adjacent to Zhanjiang Bay, which was a TDP source for the LZPCW via coastal water exchange. This bay is subjected to land-based pollutants, leading to TDP form enrichment in coastal waters (Zhang et al., 2019b; Fu et al., 2020). With the rapid industry development of Zhanjiang city, large amount of wastewater from the industrial factories with high concentrations of TDP was also discharged into the coastal water (Zhang et al., 2020a; Zhang et al., 2021). In addition,

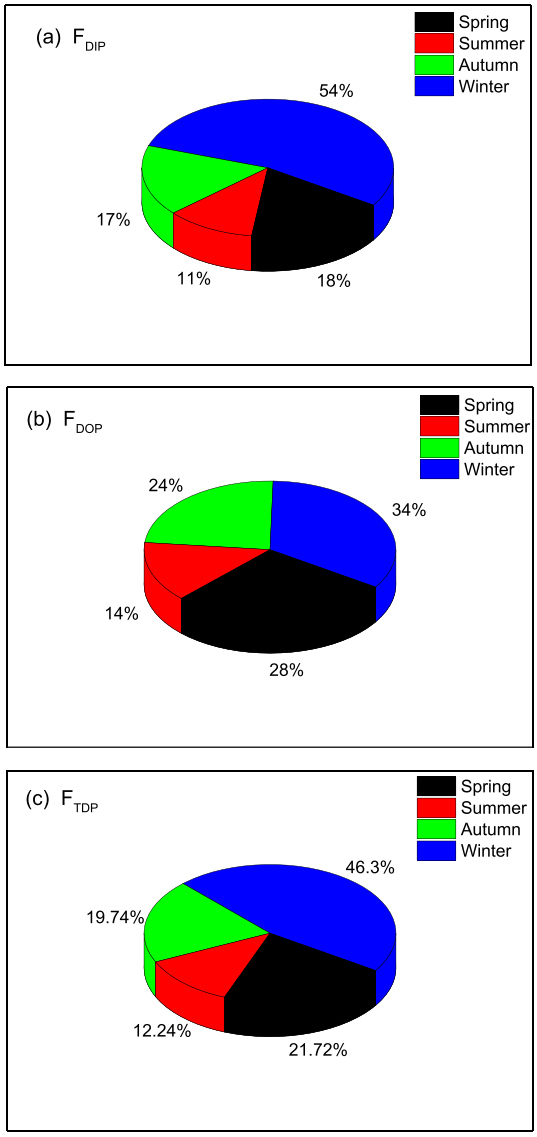

Fig. 9. Seasonal contributions of TDP flux (F_{TDP}) discharge from the QZS into the BBG.

adjacent coastal aquaculture inputs can also play a key role in TDP species variation (Xu et al., 2017; Yang et al., 2020); for example, Zhanjiang City has a large marine aquaculture industry that covered 6.5 $\times 10^4$ ha in 2016 (Zhang et al., 2020a). Moreover, the DOP concentration in coastal waters were also associated with internal sources such as the excretion of plankton and endogenous effects of marine biology in grazing between zooplankton and phytoplankton (Xu et al., 2017), which had great impacts on the TDP forms distribution pattern.

4.4. Seasonal variations affecting TDP speciation transport between the GDWCW and BBGCW

Seasonal variations in GDWCW flow discharges and concentrations of different P species were accompanied by significant changes in fluxes between the inorganic and organic phases of the TDP pool across the QZS. For DIP, DOP, and TDP, the largest fluxes occurred in winter, accounting for 54%, 34%, and 46.3%, respectively (Fig. 9). On one hand, TDP species (except DOP) had higher concentrations in winter due to the coastal water column mixed well and low biological utilization (Li et al., 2017). Similar seasonal variations in DIP were also observed in coastal waters of the Pearl River estuary and northern BBG (Guo et al., 2019; Li

et al., 2017). On the other hand, the prevailing north-eastern monsoon in winter can modulate the Pearl River estuarine coastal plume to the western part of the estuary (Dai et al., 2014), such that the GDWCW may have enriched TDP species concentrations. Winter winds could lead to a large amount of coastal water being transported to the BBG through the QZS (Gao et al., 2017; Shi et al., 2002). Outflow from the QZS may cause up to 44% of the BBGCW to be refreshed each season, suggesting that this has a significant impact on seasonal circulation in the BBG (Shi et al., 2002). Moreover, the annual DIP and DOP flux accounted for 62% and 38%, respectively, which may be attributed by the Pearl River coastal plume hydrodynamics and human activities. The Pearl River discharge water has been modified by high-intensity anthropogenic activities and enriched with DIP (Dai et al., 2014; Li et al., 2017; Chen et al., 2019). Therefore, the BBGCW was subjected to TDP species fluxes under P-limited conditions, possibly fuelling phytoplankton growth and regulating the biogeochemistry of the TDP cycle.

In spring and autumn, the TDP flux also declined due to a decrease in coastal water flow discharge from GDWCW to BBG via QZS. P transport fluxes were lowest in summer because the coastal water flow in the QZS weakened (Shi et al., 2002). The most recent observations and model results suggest that the current in the QZS flows eastward on certain days in the boreal summer (Gao et al., 2017). Additionally, the Pearl River estuarine coastal plume also changed direction to the east, which may lead to the decrease of TDP forms concentration and fluxes in coastal waters. Therefore, the transport fluxes of TDP forms in the LZPSC, through the QZS, and in the northern SCS depends on the seasonal variations in the GDWCW and the Pearl River estuarine coastal plume, the water properties of which are influenced by river discharge, discharged pollutants, rainfall, and winds.

5. Conclusions

In this study, 431 seawater samples were collected within the LZPCW from October 2017 to July 2018 to examine the seasonal variation, speciation, and transport flux of TDP and possible links to hydrographic features. TDP concentration and speciation had significant spatiotemporal variations ($P < 0.01$), with an annual mean concentration of 0.42 $\pm$ 0.25 μmol·L^{-1}. The concentration of TDP species was significantly higher in winter. Compared with other TDP species in shelf coastal waters around the world, the TDP concentration level in the study area was moderate. DIP and DOP were the main species in the TDP bulk in different seasons, comprising up to 55.5 $\pm$ 7.9% and 46.5 $\pm$ 22.6%, respectively. In addition, the BBG was subjected to an annual 3.5×10^9 mol flux of TDP through the QZS, though with significant seasonal variation. The current study reflected that coastal water currents, river plumes, and human activities were responsible for the dynamic variations in P species in the LZPSCW.

CRediT authorship contribution statement

Peng Zhang: Conceptualization, Methodology, Writing-Original draft, Reviewing and Editing, Funding acquisition. **Peidong Dai:** Methodology, Reviewing and Editing, Visualization. **Jibiao Zhang:** Methodology, Reviewing and Editing, Funding acquisition. **Jianxu Li:** Software, Data curation and Validation. **Hui Zhao:** Supervision. **Zhiguang Song:** Supervision and Funding acquisition.

Declaration of competing interest

The authors declare that they have no known competing financial interests or personal relationships that could have appeared to influence the work reported in this paper.

Acknowledgments

The authors are grateful for the anonymous reviewers' careful review and constructive suggestions to improve the manuscript. We gratefully acknowledge supported by the Research and Development Projects in Key Areas of Guangdong Province (2020B1111020004); Guangdong Basic and Applied Basic Research Foundation (2020A1515110483); Guangdong Ocean University Fund Project (R18021); Science and Technology Special Project of Zhanjiang City (2019B01081); First-class Special Fund (231419018); Innovation Strong School Project (230420007) of Guangdong Ocean University and Marine Organic Geochemistry and Climate-Environment Change (R17001).

References

Ammerman, J.W., Azam, F., 1985. Bacterial 5-nucleotidase in aquatic ecosystems: a novel mechanism of phosphorus regeneration. Science 227, 1338–1340.
Anderson, D.M., Glibert, P.M., Burkholder, J.M., 2002. Harmful algal blooms and eutrophication: nutrient sources, composition, and consequences. Estuaries 25, 704–726.
Bao, X., Hou, Y., Chen, C., Chen, F., Shi, M., 2005. Analysis of characteristics and mechanism of current system on the west coast of Guangdong of China in summer. Acta Oceanol. Sin. 24 (4), 1–9.
Benitez-Nelson, C.R., 2000. The biogeochemical cycling of phosphorus in marine systems. Earth Sci. Rev. 51, 109–135.
Bjorkman, K.S., Karl, D.M., 1994. Bioavailability of inorganic and organic phosphorus compounds to natural assemblages of microorganisms in Hawaiian coastal waters. Mar. Ecol. Prog. Ser. 111, 265–273.
Boesch, D.F., Boynton, W.R., Crowder, L.B., Diaz, R.J., Howarth, R.W., Mee, L.D., Nixon, S.W., Rabalais, N.N., Rosenberg, R., Sanders, J.G., Scavia, D., Turner, R.E., 2009. Nutrient enrichment drives Gulf of Mexico hypoxia. Eos. 90, 117–118.
Boynton, W.R., Garber, J.H., Summers, R., Kemp, W.M., 1995. Inputs, transformations, and transport of nitrogen and phosphorus in Chesapeake Bay and selected tributaries. Estuaries 18, 285–314.
Cai, W.-J., Dai, M.-H., Wang, Y.-C., Zhai, W.D., Huang, T., Chen, S.-T., Zhang, F., Chen, Z.-Z., 2004. The biogeochemistry of inorganic carbon and nutrients in the Pearl River estuary and the adjacent Northern South China Sea. Cont. Shelf Res. 24, 1301–1319.
Cai, Y., Guo, L., Wang, X., Mojzis, A.K., Redalje, D.G., 2012. The source and distribution of dissolved and particulate organic matter in the Bay of St. Louis, northern Gulf of Mexico. Estuar. Coast. Shelf Sci. 96, 96–104.
Canton, M., Anschutz, P., Poirier, D., Chassagne, R., Deborde, J., Savoye, N., 2012. The buffering capacity of a small estuary on nutrient fluxes originating from catchment (Leyre estuary, SW France). Estuar. Coast. Shelf Sci. 99, 171–181.
Chen, B., Xu, Z., Ya, H., Chen, X., Xu, M., 2019. Impact of the water input from the eastern Qiongzhou Strait to the Beibu gulf on Guangxi coastal circulation. Acta Oceanol. Sin. 38 (9), 1–11.
China Meteorological Data Service Center, 2020. Dataset of Daily Surface Observation Values in Individual Years (1981-2010) in China. http://data.cma.cn/data/weatherBk.html. 2020-5-25.
China National Standardization Management Committee, 2007. The Specification for Marine Monitoring - Part 4:Seawater Analysis. http://www.gb688.cn/bzgk/gb/newGbInfo?hcno=9FB14D0EE23D77A96D54A9BDAAF6EA07. 2021.
Conley, D.J., Smith, W.M., Cornwell, J.C., Fisher, T.R., 1995. Transformation of particle-bound phosphorus at the land-sea interface. Estuar. Coast. Shelf Sci. 40, 161–176.
Conley, D.J., Paerl, H.W., Howarth, R.W., Boesch, D.F., Seitzinger, S.P., Havens, K.E., Lancelot, C., Likens, G.E., 2009. Controlling eutrophication: nitrogen and phosphorus. Science. 323 (5917), 1014–1015.
Dagg, M., Benner, R., Lohrenz, S., Lawrence, D., 2004. Transformation of dissolved and particulate materials on continental shelves influenced by large rivers: plume processes. Cont. Shelf Res. 24, 833–858.
Dagg, M., Ammerman, J., Amon, R., Gardner, W., Green, R., Lohrenz, S., 2007. A review of water column processes influencing hypoxia in the northern Gulf of Mexico. Estuar. Coasts 30, 735–752.
Dai, M., Gan, J., Han, A., Kung, H.S., Ying, Z., 2014. Physical dynamics and biogeochemistry of the Pearl River plume. In: Bianchi, T.S., Allison, M.A., Cai, W. (Eds.), Biogeochemical Dynamics at Large River–Coastal Interfaces. Cambridge University Press, Cambridge, pp. 321–352 (Chapter 13).
Diaz, J.M., Björkman, K.M., Haley, S.T., Ingall, E.D., Karl, D.M., Longo, A.F., Dyhrman, S. T., 2016. Polyphosphate dynamics at station ALOHA, North Pacific subtropical gyre. Limnol. Oceanogr. 26, 227–2396.
Du, J.J., Zheng, C., Liao, Z.W., Wang, X.A., Yang, X.L., Li, R.M., 2004. Technique of high efficient utilization of phosphoric fertilizer and its application in Leizhou peninsula. Ecol. Environ. 13 (3), 373–375.
Duan, L.Q., Song, J.M., Yuan, H.M., Li, X.G., Li, N., 2016. Distribution, partitioning and sources of dissolved and particulate nitrogen and phosphorus in the north Yellow Sea. Estuar. Coast. Shelf Sci. 181, 182–195.
Eppley, R.W., 1972. Temperature and phytoplankton growth in the sea. Fish. Bull. Nat. Ocean. Atmos. Adm. 70, 1063–1085.
Fang, T., 2004. Phosphorus speciation and budget of the east China sea. Cont. Shelf Res. 24, 1285–1299.
Fang, T.H., 2000. Partitioning and behavior of different forms of phosphorus in the Tanshui Estuary and one of its tributaries. Northern Taiwan. Estuar. Coast. Shelf Sci. 50, 689–701.

Fang, T.H., Wang, C.W., 2020. Dissolved and particulate phosphorus species partitioning and distribution in the Danshuei River Estuary, Northern Taiwan. Mar. Pollut. Bull. 151, 110839.
Faul, K.L., Paytan, A., Delaney, M.L., 2005. Phosphorus distribution in sinking oceanic particulate matter. Mar. Chem. 97, 307–333.
Fox, L.E., Sager, S.L., Wofsy, S.C., 1986. The chemical control of soluble phosphorus in the Amazon estuary. Geochim. Cosmochim. Acta 50, 783–794.
Froelich, P.N., 1988. Kinetic control of dissolved phosphate in natural rivers and estuaries: a primer on the phosphate buffer mechanism. Limnol. Oceanogr. 33, 649–668.
Fu, D., Zhong, Y., Chen, F., Yu, G., Zhang, X., 2020. Analysis of dissolved oxygen and nutrients in Zhanjiang Bay and the adjacent sea area in spring. Sustainability 12 (3), 889.
Gao, J., Wu, G., Ya, H., 2017. Review of the circulation in the Beibu Gulf, south China Sea. Cont. Shelf Res. 138, 106–119.
Glibert, P.M., 2017. Eutrophication, harmful algae and biodiversity - challenging paradigms in a world of complex nutrient changes. Mar. Pollut. Bull. 124 (2), 591–606.
Grasshoff, K., Kremling, K., Ehrhardt, M., 1999. Methods of Seawater Analysis. Weinheim, Wiley-VCH, pp. 200–208.
Guo, J., Wang, Y., Lai, J., Pan, C., Wang, S., Fu, H., Zhang, B., Cui, Y., Zhang, L., 2019. Spatiotemporal distribution of nitrogen biogeochemical processes in the coastal regions of northern Beibu Gulf, south China Sea. Chemosphere 239, 124803.
Hansell, D.A., Carlson, C.A. (Eds.), 2014. Biogeochemistry of Marine Dissolved Organic Matter. Chapter 5: Dynamics of Dissolved Organic Phosphorus. Academic Press, pp. 127–212.
Howarth, R.W., Jensen, H.S., Marino, R., Postma, H., 1995. Transport to and processing of P in near-shore and oceanic waters. In: Tiessen, H. (Ed.), Phosphorus in the Global Environment. Transfers, Cycles and Management. Wiley, West Sussex, pp. 323–346.
Huang, X.L., Zhang, J.Z., 2010. Spatial variation in sediment-water exchange of phosphorus in Florida bay: AMP as amodel organic compound. Environ. Sci. Technol. 44, 7790–7795.
Jiang, S.C., 2008. Study on speciation and distribution of phosphorus in water and surface sediments of Beibu Gulf in summer. M.S. Thesis. Xiamen University, Xiamen, China. 28–29.
Karl, D., Björkman, K.M., 2001. Phosphorus cycle in seawater: dissolved and particulate pool inventories and selected phosphorus fluxes. Methods Microbiol. 30, 239–270.
Kolowith, L.C., Ingall, E.D., Benner, R., 2001. Composition and cycling of marine organic phosphorus. Limnol. Oceanogr. 46 (2), 309–320.
Koroleff, F., 1983. Determination of phosphorus. In: Grasshoff, K., Kremling, K., Ehrhardt, M. (Eds.), Methods of Seawater Analysis. Verlag Chemie, pp. 167–173.
Li, F., Lin, J., Liang, Y., Gan, H., Zeng, X., Duan, Z., Liang, K., Liu, X., Huo, Z., Wu, C., 2014. Coastal surface sediment quality assessment in Leizhou peninsula (South China Sea) based on SEM-AVS analysis. Mar. Pollut. Bull. 84 (1–2), 424–436.
Li, R., Xu, J., Li, X., Shi, Z., Harrison, P.J., 2017. Spatiotemporal variability in phosphorus species in the Pearl River estuary: influence of the river discharge. Sci. Rep. 7.
Lin, P., Chen, M., Guo, L.D., 2012. Speciation and transformation of phosphorus and its mixing behavior in the Bay of St. Louis estuary in the northern Gulf of Mexico. Geochim. Cosmochim. Ac. 87, 283–298.
Lin, P., Guo, L., Chen, M., Cai, Y., 2013. Distribution, partitioning and mixing behavior of phosphorus species in the Jiulong River estuary. Mar. Chem. 157, 93–105.
Liu, S.M., Li, L.W., Zhang Z., 2011. Inventory of nutrients in the Bohai. Cont. Shelf Res. 31(16):0–1797.
Loh, A.N., Bauer, J.E., 2000. Distribution, partitioning and fluxes of dissolved and particulate organic C, N and P in the eastern North Pacific and Southern Oceans. Deep-Sea Res. I 47, 2287–2316.
Mather, R.L., Reynolds, S.E., Wolff, G.A., Williams, R.G., Torres-valdes, S., Woodward, E. M., Landolfi, A., Pan, X., Sanders, R., Achterberg, E., 2008. Phosphorus cycling in the North and South Atlantic Ocean subtropical gyres. Nat. Geosci. 1, 439–443.
Meng, J., Yu, Z., Yao, Q., Bianchi, T.S., Paytan, A., Zhao, B., Pan, H., Yao, P., 2015. Distribution, mixing behavior, and transformation of dissolved inorganic phosphorus and suspended particulate phosphorus along a salinity gradient in the Changjiang estuary. Mar. Chem. 168, 124–134.
Orrett, K., Karl, D.M., 1987. Dissolved organic phosphorus production in surface seawaters. Limnol. Oceanogr. 32, 383–395.
Pang, H.L., 2006. Analysis of diffuse route of Zhujiang River diluted water. M.S. Thesis. Ocean University of China, Qingdao, China, pp. 3–4.
Raimbault, P., Pouvesle, W., Diaz, F., Garcia, N., Sempéré, R., 1999. Wet-oxidation and automated colorimetry for simultaneous determination of organic carbon, nitrogen and phosphorus dissolved in seawater. Mar. Chem. 66, 61–169.
Ridal, J.J., Moore, R.M., 1990. A re-examination of the measurement of dissolved organic phosphorus in seawater. Mar. Chem. 29, 19–31.
Shi, M.C., Chen, C.S., Xu, Q., Lin, H., Liu, G., Wang, H., Wang, F., Yan, J., 2002. The role of Qiongzhou Strait in the seasonal variation of the South China Sea circulation. J. Phys. Oceanogr. 32, 103–12129.
Shi, Y., Zhang, Y., Sun, X., 2015. Spatiotemporal distribution of eutrophication and its relationship with environmental factors in Zhanjiang sea bay area. Environ. Sci. Technol. 38, 90–96.
van der Zee, C., Roevros, N., Chou, L., 2007. Phosphorus speciation, transformation and retention in the Scheldt estuary (Belgium/the Netherlands) from the freshwater tidal limits to the North Sea. Mar. Chem. 106, 76–91.
Xie, L.L., Cao, R.X., Shang, Q.T., 2012. Progress of study on coastal circulation near the shore of western Guangdong. J Guangdong Ocean U. 32 (04), 94–98.
Xu, C., Dan, S.F., Yang, B., Lu, D.L., Kang, Z.J., Huang, H.F., Zhou, J.D., Ning, Z.M., 2021. Biogeochemistry of dissolved and particulate phosphorus speciation in the Maowei Sea, northern Beibu gulf. J. Hydrol. 593, 125822.
Xu, J., Yin, K., He, L., Yuan, X., Ho, A.Y.T., Harrison, P.J., 2008. Phosphorus limitation in the northern South China Sea during late summer: influence of the Pearl River. Deep-Sea Res. I 55 (10), 1330–1342.
Xu, W., Li, R., Liu, S., Ning, Z., Jiang, Z., 2017. The phosphorus cycle in the Sanggou Bay. Acta Oceanol. Sin. 36, 90–100.
Yang, B., Kang, Z., Lu, D., Dan, S.F., Ning, Z., Lan, W., Zhong, Q., 2018. Spatial variations in the abundance and chemical speciation of phosphorus across the river–sea interface in the northern Beibu gulf. Water 10 (8), 1103.
Yang, B., Gao, X., Zhao, J., Lu, Y., Gao, T., 2020. Biogeochemistry of dissolved inorganic nutrients in an oligotrophic coastal mariculture region of the Northern Shandong Peninsula, North Yellow Sea. Mar. Pollut. Bull. 150, 110693.
Yang, Y., Rui-Xiang, L.I., Peng-Li, Z., Pin-De, R., 2014. Seasonal variation of the pearl river diluted water and its dynamical cause. Mar. Sci. Bull. 33 (1), 36–44.
Yang, Y., Xu, Y.D., Wang, X., F.Y., Wei, X., 2015. A numerical hydrodynamic and transport model in the West Coast of Guangdong Province. Sci. Technol. Eng. 19, 86–91.
Zhang, J.B., Zhang, P., Dai, P.D., Lai, J.Y., Chen, Y., 2019a. Spatiotemporal distributions of DIP and the eutrophication in Hainan Island adjacent coastal water. China Environ. Sci. 39 (6), 2541–2548.
Zhang, J.B., Zhang, Y.C., Zhang, P., Li, Y., Li, J.X., Xu, J.L., Luo, X.Q., Zhao, L.R., 2021. Seasonal phosphorus variation in coastal water affected by the land-based sources input in the eutrophic Zhanjiang Bay, China. Estuar. Coast. Shelf Sci. 252, 107277.
Zhang, P., Wei, L.R., Lai, J.Y., Dai, P.D., Chen, Y., Zhang, J.B., 2019b. Concentration, composition and fluxes of land-based nitrogen and phosphorus source pollutants input into Zhanjiang Bay in summer. J Guangdong Ocean U. 39 (4), 46–55.
Zhang, P., Peng, C.H., Zhang, J.B., Zou, Z.B., Shi, Y.Z., Zhao, L.R., Zhao, H., 2020a. Spatiotemporal urea distribution, sources, and indication of DON bioavailability in Zhanjiang Bay, China. Water 12 (3), 633.
Zhang, P., Ruan, H.M., Dai, P.D., Zhao, L.R., Zhang, J.B., 2020b. Spatiotemporal river flux and composition of nutrients affecting adjacent coastal water quality in Hainan Island, China. J. Hydrol. 591, 125293.
Zhanjiang City Government, 2013. Zhanjiang City Records.